

## Structural origin of the intermediate phase in Ge–Se glasses

G. Chen,<sup>a)</sup> F. Inam, and D. A. Drabold

*Department of Physics and Astronomy, Ohio University, Athens, Ohio 45701, USA*

(Received 20 July 2010; accepted 9 September 2010; published online 27 September 2010)

We have conducted x-ray absorption near-edge structure (XANES) experiments on germanium selenide glasses, in search of a structural signature of the intermediate phase (IP). Quantitative analyses of the XANES spectra reveal compositional plateaus that coincide with the IP reversibility window, providing structural evidence for the IP. Molecular dynamic simulations have been performed to understand the atomistic origin of the electronic structure of the glasses. The IP originates from a competition between amorphous GeSe<sub>2</sub> and amorphous Se clusters and produces measurable signatures. Our study provides atomistic insight into the structural origin of the IP in Ge–Se glasses. © 2010 American Institute of Physics. [doi:10.1063/1.3495775]

Glasses are nonequilibrium solids formed by rapid cooling of liquids. In a binary or multielement glass system, different elastic phases could exist. Phillips<sup>1</sup> and Thorpe<sup>2</sup> predicted three decades ago that floppy and rigid phases exist in covalent glass systems, and a floppy-to-rigid transition occurs at a composition that has an average coordination number of 2.4. This solitary-transition theory was not questioned until two decades later when Boolchand first provided evidence that instead of a single-composition phase transition, double transitions exist due to a third phase with a range of compositions sandwiched between the floppy and the rigid phases. The third phase was named the intermediate phase (IP). An important property of the IP lies in its nearly non-hysteretic glass transition behavior, characterized by an almost vanishing nonreversing heat flow. Consequently, the IP compositional window is also called the reversibility window.

Since its first discovery over a decade ago, the IP has been identified in many glass systems,<sup>3</sup> mostly through two experimental methods: Raman spectroscopy and temperature-modulated differential scanning calorimetry.<sup>4</sup> In spite of the spectroscopic and thermodynamic evidence, the atomistic origin of the IP has been elusive.<sup>5–7</sup> Searches for direct structural evidences of the IP have been conducted by a few research groups.<sup>8–10</sup> Wang,<sup>8</sup> Sharma,<sup>9</sup> and their co-workers studied the Ge–Se glasses using x-ray diffraction. They found that the area and the inverse position of the first sharp diffraction peak exhibited a compositional plateau that matched the reversibility window of the IP, implying a correlation between the intermediate range order (IRO) and the IP. However, a similar study by Shatnawi and co-workers could not confirm this observation.<sup>10</sup> The latter paper also reported extended x-ray absorption fine structure analysis of the Ge–Se glasses and found no correlation between the short-range order and the IP. This controversy is partly due to the fact that the local structure of the Ge–Se glasses is rather complex. For instance, Se-77 NMR studies of the Ge–Se glasses have been interpreted in markedly different ways.<sup>11,12</sup>

In this paper, we report an x-ray absorption near-edge structure (XANES) study of the Ge–Se glasses including the IP compositions. XANES contains information about the atomic and electronic structure of materials and is usually

more sensitive than the extended x-ray absorption fine structure on an intermediate length scale ( $\sim$ several angstroms). Our quantitative analyses of the XANES spectra reveal that both the electronic and the intermediate-range structures exhibit the telltale composition plateau that coincides with the IP reversibility window. Our study sheds light on the structural origin of the IP in Ge–Se glasses.

Binary Ge<sub>x</sub>Se<sub>100-x</sub> glasses ( $x=18, 19, 21, 23, 24, 27, 30$ ) were prepared by the traditional melt-quenching method by the Boolchand group.<sup>13</sup> The selected compositions encompass the IP window ( $x \approx 20–25$ ). Ge and Se K-edge XANES experiments were performed in transmission mode at the Advanced Photon Source (APS), Argonne National Laboratory. Bulk Ge–Se glasses were ground into fine powders and then spread evenly onto kapton tape. Four to eight layers of such tape were stacked together to optimize the signal-to-noise ratio. The powder samples were freshly prepared just before the XANES experiments to minimize contact with air. A Ge<sub>30</sub>Se<sub>70</sub> powder sample was used as a reference to calibrate the absorption edges for all the samples.

Molecular dynamics (MD) simulations have been performed to derive the electronic structures of the germanium selenide glasses. Details of the atomic models are described elsewhere.<sup>14,15</sup> The focus of the MD simulations is on the correlation between the atomic structure and the conduction band structure of the glasses.

Figure 1(a) shows the normalized Se K-edge XANES spectra of selected Ge<sub>x</sub>Se<sub>100-x</sub> glasses. The compositions  $x=18$ ,  $x=21$  and  $24$ , and  $x=30$  correspond to the floppy, intermediate, and rigid phases, respectively. A strong absorption peak (located at  $\sim 12659$  eV) is observed in the XANES spectra. This peak originates from the electronic transition between the core  $1s$  orbital and the unoccupied electronic states (viz., the conduction band) and is called the white line (WL).<sup>16</sup> Intensity of the WL is an indication of the electronic density of unoccupied states in the conduction band. Two features in the WL are observed to change with  $x$ . The first one is a peak located at  $\sim 12659$  eV [its expanded view is shown in the inset of Fig. 1(a)]. The intensity of this peak decreases as the glass evolves from the floppy phase ( $x=18$ ) to the intermediate phase ( $x=21, 24$ ), and it hardly changes within the IP compositions. Further increase in  $x$  leads to a lower intensity and the glass becomes a rigid phase ( $x=30$ ). The second feature is a hidden peak located near the

<sup>a)</sup>Electronic mail: cheng3@ohio.edu.

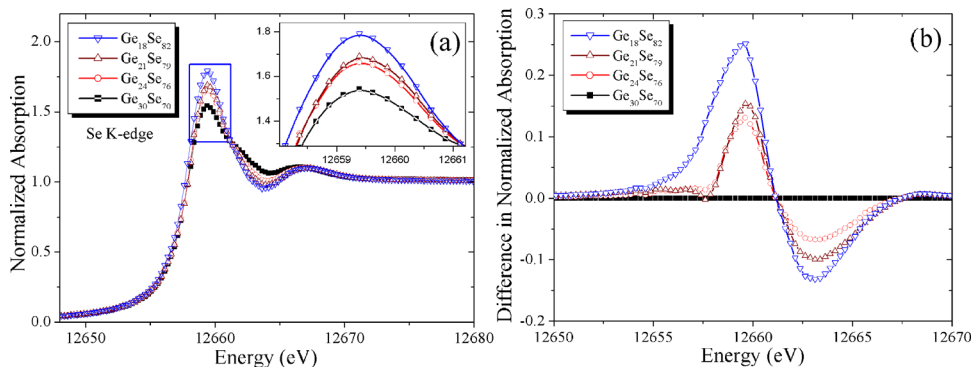


FIG. 1. (Color online) (a) Normalized Se K-edge XANES spectra of selected  $\text{Ge}_x\text{Se}_{100-x}$  ( $x=18, 21, 24,$  and  $30$ ) glasses, including the floppy ( $x=18$ ), intermediate ( $x=21, 24$ ), and rigid ( $x=30$ ) phases; (b) The difference XANES spectra of the four glasses (with respect to the  $\text{Ge}_{30}\text{Se}_{70}$  glass).

tail of the WL (at  $\sim 12663$  eV), and its intensity increases continuously with  $x$ . After taking difference spectra with respect to the  $\text{Ge}_{30}\text{Se}_{70}$  spectrum, we cancel out the edge jump caused by the absorption edge so that the two peaks in the WL can be clearly seen. Figure 1(b) shows the difference spectra of the four glasses, where the two peaks are measured to be  $\sim 3.5$  eV apart. Quantitative analysis of these two peaks results in a plot of the difference peak areas as a function of Ge content (Fig. 2). For the first (left) peak, its area decreases as the glass transits from the floppy phase to the rigid phase. A plateau is observed between  $x=21$  and  $24$ , which overlaps with the IP window. In contrast, the area of the second (right) peak increases almost linearly with  $x$  and thus does not show a similar compositional plateau.

We also conducted a Ge K-edge XANES experiment on the  $\text{Ge}_x\text{Se}_{100-x}$  glasses. Figure 3(a) shows normalized XANES spectra of selected compositions ( $x=18, 21, 24, 30$ ). A strong WL appears at  $\sim 11107$  eV, followed by a shoulder that is peaked at  $\sim 11113$  eV. The profile of the WL does not show any composition dependence within experimental uncertainty. However, the shoulder does show such a dependency, which can be seen from the inset of Fig. 3(a). The intensity of the shoulder decreases as the glass moves from the floppy phase to the rigid phase, but it changes little within the intermediate phase. Figure 3(b) shows a plot of the relative area under the shoulder as a function of  $x$ . The shoulder area decreases as the glass evolves from the floppy phase to the rigid phase, but it remains a constant within the

IP compositions. The observed compositional plateau provides additional evidence for the IP.

In the Se-rich  $\text{Ge}_x\text{Se}_{100-x}$  glasses ( $x < 33$ ), the chemical environment around Ge is expected to be composition independent, i.e., each Ge bonds to four Se to form a  $\text{GeSe}_2$  tetrahedron. We observe that the WL of the Ge XNAES spectra is composition independent (for  $x \leq 30$ ), which implies that the WL is strongly related to the chemical environment but is insensitive to the arrangement of the  $\text{GeSe}_2$  tetrahedra. In contrast, the shoulder after the Ge K-edge WL shows a composition dependency and thus is related to the arrangement of the  $\text{GeSe}_2$  tetrahedra. It is known that the IRO of glasses is related to the arrangement of polyhedral building blocks (e.g., in the Ge–Se glasses, the ways to connect adjacent  $\text{GeSe}_2$  tetrahedra through corner or edge sharing).<sup>17</sup> Therefore, the observed shoulder in the Ge XNAES spectra is a signature of the IRO. The area under the shoulder shows a composition plateau overlapping with the IP window, which implies that the IRO barely changes for the IP glasses. Raman study of the Ge–Se glasses has shown that the vibration frequency of the corner-sharing  $\text{GeSe}_2$  tetrahedra remains a constant within the IP composition window.<sup>4</sup> Since the corner sharing is an important component of the IRO, our Ge K-edge XANES result resonates with the finding from the Raman study.

To understand the structural origin behind the observed compositional plateau in Fig. 2, it is useful to correlate the conduction band structure with the atomic structure. For this purpose, we have conducted *ab initio* MD simulations on  $\text{Ge}_x\text{Se}_{100-x}$  ( $x=10, 15, 18, 20, 22, 23, 25, 33$ ) glasses. Details of the computer models can be found elsewhere.<sup>14,15</sup> The simulated conduction bands of all the compositions consist of two major peaks, which are approximately 3.5 eV apart and thus consistent with the WL features in the Se XANES spectra (Fig. 1). Projection of the unoccupied electronic density of states onto the Se-related structural units reveals that the first peak (i.e., the one at lower energy) is contributed by Se–Se–Se, Se–Se–Ge, and Ge–Se–Ge with weighing factors in the order of Se–Se–Se > Se–Se–Ge > Ge–Se–Ge. In contrast, the second peak in the WL is dominated by the contribution from the Ge–Se–Ge units. From the composition dependency of the Ge K-edge WL [Fig. 3(a)], we know that intensity of the WL is strongly related to the ratio between the number of individual structural units and the total number of possible structural units. In the case of the Ge WL, this ratio is  $\sim 1$  for all the compositions ( $x \leq 30$ ). Therefore, the WL intensity does not change with  $x$ . For the second peak of the Se WL, we observe that the area under the peak increases linearly with  $x$  (Fig. 2), suggesting that the fraction

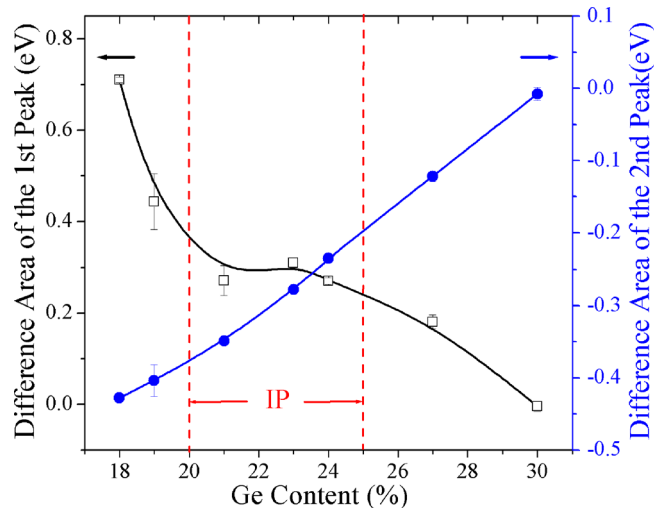


FIG. 2. (Color online) The difference areas of the 1st and 2nd peak of the Se WL as a function of Ge content. The dashed lines indicate the boundaries of the IP reversibility window. The solid curves are guides to the eye.

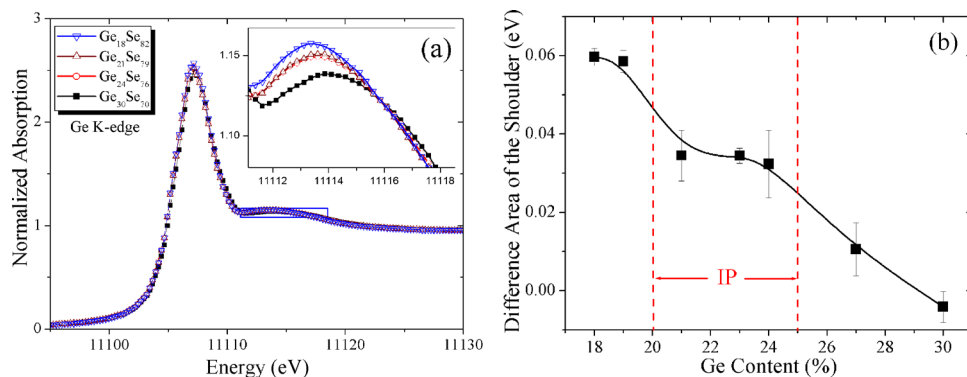


FIG. 3. (Color online) (a) Normalized Ge K-edge XANES spectra of selected  $\text{Ge}_x\text{Se}_{100-x}$  ( $x=18, 21, 24,$  and  $30$ ) glasses, including the floppy ( $x=18$ ), intermediate ( $x=21, 24$ ), and rigid ( $x=30$ ) phases; (b) The difference area of the shoulder of the Ge WL as a function of Ge content. The dashed lines indicate the boundaries of the IP reversibility window. The solid curve is a guide to the eye.

of Ge–Se–Ge units is a linear function of  $x$ . This composition dependency has been predicted previously by the MD simulations.<sup>14</sup> Since the Ge–Se–Ge units correspond to the corner- and edge-sharing  $\text{GeSe}_2$  tetrahedra, the observed linear increase in the fraction of Ge–Se–Ge means *growth* of the amorphous  $\text{GeSe}_2$  tetrahedral clusters as  $x$  increases. In other words, as we add more and more Ge into the glass, the subsequently formed  $\text{GeSe}_2$  tetrahedra prefer attaching to the existing  $\text{GeSe}_2$  tetrahedra rather than being isolated from them.

The first peak of the Se WL shows a composition plateau that overlaps with the IP window (Fig. 2). This peak is contributed by the Se–Se–Se, Se–Se–Ge, and Ge–Se–Se units as suggested by our MD simulations. The Ge–Se–Ge species represents the amorphous  $\text{GeSe}_2$  cluster, and its concentration increases linearly with  $x$  as confirmed by both the XANES experiment and the MD simulations. The Se–Se–Se species represents the amorphous Se phase, and its concentration decreases linearly with  $x$  as indicated by the MD simulations.<sup>14</sup> Since the weighting factor of Se–Se–Se units for the first peak of the Se WL is larger than that of the Ge–Se–Ge units, a sum of these two linear functions produces another linear function with a negative slope. However, these two structural species alone cannot explain the kink in the IP window [Fig. 2(b)]. Therefore, the third structural species (i.e., Se–Se–Ge) should be responsible for the observed compositional plateau. MD simulations show that the concentration profile of Se–Se–Ge has a maximum plateau inside the IP composition window.<sup>14</sup> Such a composition dependency of the Se–Se–Ge units should explain the “kink” in the IP window as observed from our XANES experiment. The Se–Se–Ge units link both the Se clusters and the  $\text{GeSe}_2$  clusters and thus represent the interface between these two types of clusters. Concentration of the Se–Se–Ge units is proportional to the interfacial area, which reaches a maximum plateau within the IP window. This plateau implies that the a- $\text{GeSe}_2$  clusters have a maximum degree of contact with the a-Se clusters. Further increase in the Ge content causes the  $\text{GeSe}_2$  clusters to merge and thus a decrease in the interfacial area is expected for the rigid phase.

Based on the combined experimental and theoretical results, an atomistic picture of the Ge–Se glasses is proposed for their structural evolution from the floppy phase to the rigid phase. In a floppy  $\text{Ge}_x\text{Se}_{100-x}$  ( $x < 20$ ) glass, the minority a- $\text{GeSe}_2$  clusters are well dispersed in the a-Se matrix with the Se–Se–Ge units holding these two phases together. Here we call the a- $\text{GeSe}_2$  clusters “nuclei.” As we add more Ge into the glass system, the subsequently added Ge prefers to attach to the existing nuclei, causing them to grow at the

expense of the a-Se clusters. As we keep adding Ge into the system, the glass enters the IP region where the surface area of the nuclei reaches a maximum plateau. At this point, these nuclei are still separated from each other by the a-Se clusters, which become shorter and shorter because of the consumption by subsequently added Ge. This process causes the concentration of short-chain Se to reach a maximum plateau in the IP window as confirmed by the MD simulations.<sup>15</sup> Further increase in the Ge concentration results in merging of the nuclei, so the total surface area of the nuclei starts to decrease. Therefore, formation of the IP is caused by clustering of the  $\text{GeSe}_2$  tetrahedra and, more importantly, a competition between the a- $\text{GeSe}_2$  and a-Se phases. Our study proves that XANES is a very useful tool for investigating the IP of glasses.

The authors would like to thank Professor Boolchand for providing the samples and T. Bolin, Q. Ma, K. Li, B. Prasai, and V. Thota for assisting the experiment. Use of the APS was supported by the DOE-BES under Contract No. DE-AC02-06CH11357. This work was supported by the NSF under Grant Nos. DMR-0906825 (to G. Chen) and DMR-0902936 (to D. A. Drabold).

<sup>1</sup>J. C. Phillips, *J. Non-Cryst. Solids* **34**, 153 (1979).

<sup>2</sup>M. F. Thorpe, *J. Non-Cryst. Solids* **57**, 355 (1983).

<sup>3</sup>M. Micoulaut and J. C. Phillips, *J. Non-Cryst. Solids* **353**, 1732 (2007).

<sup>4</sup>P. Boolchand, X. Feng, and W. J. Bresser, *J. Non-Cryst. Solids* **293–295**, 348 (2001).

<sup>5</sup>M. F. Thorpe, D. J. Jacobs, M. V. Chubynsky, and J. C. Phillips, *J. Non-Cryst. Solids* **266–269**, 859 (2000).

<sup>6</sup>M. Micoulaut and J. C. Phillips, *Phys. Rev. B* **67**, 104204 (2003).

<sup>7</sup>P. Boolchand, D. G. Georgiev, and B. Goodman, *J. Optoelectron. Adv. Mater.* **3**, 703 (2001).

<sup>8</sup>Y. Wang, E. Ohata, S. Hosokawa, M. Sakurai, and E. Matsubara, *J. Non-Cryst. Solids* **337**, 54 (2004).

<sup>9</sup>D. Sharma, S. Sampath, N. P. Lalla, and A. M. Awasthi, *Physica B* **357**, 290 (2005).

<sup>10</sup>M. T. M. Shatnawi, C. L. Farrow, P. Chen, P. Boolchand, A. Sartbaeva, M. F. Thorpe, and S. J. L. Billinge, *Phys. Rev. B* **77**, 094134 (2008).

<sup>11</sup>P. Lucas, E. A. King, O. Gulbilen, J. L. Yarger, E. Soignard, and B. Bureau, *Phys. Rev. B* **80**, 214114 (2009).

<sup>12</sup>E. L. Gjersing, S. Sen, and B. G. Aitken, *J. Phys. Chem. C* **114**, 8601 (2010).

<sup>13</sup>F. Wang, S. Mamedov, P. Boolchand, B. Goodman, and M. Chandrasekhar, *Phys. Rev. B* **71**, 174201 (2005).

<sup>14</sup>F. Inam, M. T. Shatnawi, D. Tafen, S. J. L. Billinge, P. Chen, and D. A. Drabold, *J. Phys.: Condens. Matter* **19**, 455206 (2007).

<sup>15</sup>F. Inam, D. N. Tafen, G. Chen, and D. A. Drabold, *Phys. Status Solidi B* **246**, 1849 (2009).

<sup>16</sup>D. C. Koningsberger and R. Prins, *X-ray absorption: Principles, Applications, Techniques of EXAFS, SEXAFS and XANES* (Wiley, New York, 1988), p. 618.

<sup>17</sup>G. N. Greaves and S. Sen, *Adv. Phys.* **56**, 1 (2007).